PROC. OF JSCE
No. 322, June 1982

FATIGUE OF LARGE-SIZED LONGITUDINAL BUTT WELDS WITH PARTIAL PENETRATION

By Chitoshi MIKI, Jiro TAJIMA**, Kazuo ASAHI***, Hiroyuki TAKENOUCHI*****

1. INTRODUCTION

The Kobe-Naruto and Kojima-Sakaide routes of the Honshu-Shikoku bridges are designed to be of the combination railway and highway type. Consequently, fatigue due to live loads will pose a problem of grave importance. The allowable fatigue stresses employed in the designs of Honshu-Shikoku bridges have been determined on the basis of results of tests on various joint specimens as indicated in [1]. However, the configurations and dimensions of specimens in fatigue tests performed in the past were fairly restricted due to limitations in the capacities of testing machines, and considering the scales of the bridges, it is necessary to examine fatigue properties of various joints using larger specimens.

Accordingly, the Honshu-Shikoku Bridge Authority has had a fatigue testing machine of the capacity of maximum dynamic load of 400 ton [4×10^6 N] made and is now carrying out fatigue tests of joints and parts of structures. In the present study, fatigue properties of the partially penetrated longitudinal welded members were examined experimentally using specimens of 800-N/mm^2 class high tensile strength steel 45 mm in thickness. Plates 45-mm thick will generally be used in Honshu-Shikoku bridges.

For railway bridges in Japan[1] the allowable fatigue stress for this type of joint is that for the highest strength group, Category A: 15.3 kg/mm^2 (150 N/mm^2) under pulsating stress. Adoption of the same value had been considered for the Honshu-Shikoku bridges[2]. However, in fatigue tests of panel point structures of trusses[3),4)], fatigue cracks were initiated at corner welds of box section truss members after only a small number of repetitive stresses which were not more than the above-mentioned allowable stress. Consequently, for the Honshu-Shikoku bridges, this joint is classified today as Category B (12.75 kg/mm^2 (125 N/mm^2) under pulsating stress)[5].

Previous fatigue studies by the authors et. al. on common-size single-bevel groove weld specimens have clarified that the reduction in fatigue strength due to existence of welding residual stress is very substantial[6),7)] and that fatigue cracks are initiated from bottom surfaces of weld metal at extremely early stages of the lives[8]. Studies by Ito et al.[9] on the same kind of joint suggested that fatigue strength of this joint decreases as the size of the specimen is enlarged, and therefore, it is important for prevention of fatigue failure of steel members that the fatigue properties of this joint indicated by small-size specimens be confirmed with large specimens.

2. WELD FABRICATION AND TESTING METHOD

The steel for testing was 80-kg/mm^2 [800 N/mm^2] class quenched and tempered high tensile strength steel of 45-mm thickness, the mechanical properties and chemical composition of which are shown in **Table 1**. Welding was done by the automatic submerged-arc welding process [electrode: US80B 4.8 ϕ, flux: MF38]. Tack welds were made manually [electrode: LB52, 5 ϕ] at the middles and other specified locations of specimens. The welding detail is shown in **Fig. 1** and the welding conditions are shown in **Table 2**. The configurations and dimensions of the specimens are indicated in **Fig. 2**, these consisting of

* Member of JSCE, Dr. of Engineering, Associate Professor, Dept. of Civil Engineering, Faculty of Engineering, Tokyo Institute of Technology
** Member of JSCE, Dr. of Engineering, Professor, Dept. of Construction Engineering, Faculty of Engineering, Saitama University (formerly: Honshu-Shikoku Bridge Authority)
*** Member of JSCE, Head, Mukaishima Construction Office, Honshu-Shikoku Bridge Authority
**** Member of JSCE, Researcher, Japan Construction Method and Machinery Research Institute

Table 1 Mechanical Properties and Chemical Composition.

Mechanical Properties				Composition (%)								
Yield Point kg/mm² (N/mm²)	Tensile Strength kg/mm² (N/mm²)	Elongation %	Impact Test VE-15° kg·m (N. m)	C ×100	Si ×100	Mn ×100	P ×1000	S ×1000	Ni ×100	Cr ×100	Mo ×100	B ×1000
77 (755)	84 (823)	24	20.5 (201)	10	27	97	15	5	104	59	33	2

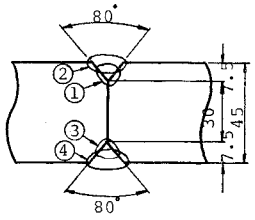

Fig. 1 Welding Detail.

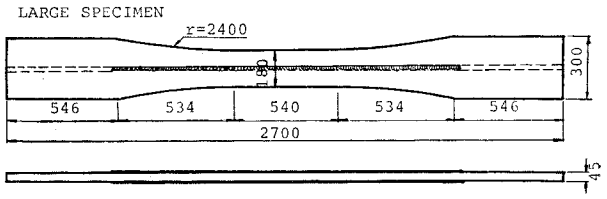

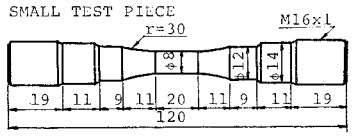

Fig. 2 Configurations and Dimensions of Specimen.

Table 2 Welding Conditions.

Number of Pass	Current (A)	Voltage (V)	Travel Speed (cm/min)
1	700	33	30
2	700	40	30
3	700	33	30
4	700	40	30

Interpass temperature: 150°C

a large specimen having a plate width at the parallel portion of 180 mm and thickness of 45 mm, and a small test piece having a parallel portion of diameter of 8 mm cut out from the welded portion of one large specimen.

Fatigue tests of large specimens were performed using a servo type fatigue testing machine of the Honshu-Shikoku Bridge Authority having a maximum dynamic loading amplitude of 400 ton (4×10^6 N). A servo type fatigue testing machine capable of applying maximum dynamic load of 5.0 ton (5×10^4 N) was used for fatigue tests of small test pieces. The fatigue tests of large specimens and small test pieces were performed with pulsating loads of minimum stresses of approximately 0.1 kg/mm² (1 N/mm²) for the former and 1 kg/mm² (10 N/mm²) for the latter. The load waveformes were sine waves for both. While further, in order to clarify the initiation and propagation properties of fatigue cracks, beach mark tests were performed.

The welding residual stresses of large specimens were obtained by the method of pasting strain gages (gage length 2 mm) on the test section and measuring the released strain when a small piece was cut with a saw. Measurements were made on one unloaded large specimen and one large specimen after fatigue test. The welding residual stresses of small test pieces were almost completely relieved since the test pieces were cut out from weld portions.[6),7),8)]

3. RESULTS OF FATIGUE TESTS

The results of all fatigue tests are listed in **Table 3**. With seven of the entire nine large specimens tested for fatigue, fatigue cracks were initiated from blowwholes existing at weld roots, and with three out of six specimens, locations of fatigue crack initiation were in portions of tack welds. The size of blowholes in the **Table 3** are the length and width of that. **Photo 1** shows the example of blowhole in fracture surface from which fatigue crack was initiated.

Photo. 2 is the example of fracture planes which was ruptured along the weld lines of the portions of tack weld of large specimens after fatigue testing. In all of the specimens, penetration into grooves was sufficient and tack welds were remelted by succeeding welds, and consequently, the configurations of welding lines were regular and smooth. However, there were a few small blowholes at weld roots. The occurrence of blowholes was remarkable especially in the portions of tack welds. The locations of fatigue crack

Table 3 Fatigue Test Results.

		Stress Range S kg/mm² (N/mm²)	Failure Life N_f cycles ($\times 10^3$)	Locations of Fatigue Crack Initiation	Size of Blowhole (mm)
Large Specimen	T-1	25.2 (247)	1 762	Surface	
	T-2	25.0 (245)	1 249	Root (blowhole)	0.8×1.3
	T-3	27.2 (267)	527	Root (blowhole)	1.3×1.9
	T-4	22.4 (220)	555	Surface (pit of weld metal)	
	T-5	22.7 (222)	1 224	Root (blowhole)	0.2×1.8
	T-7	20.1 (197)	2 567	Root (blowhole)	0.8×1.0
	T-8*	22.0 (216)	1 708	Root (blowhole)	0.6×0.4
	T-9*	27.2 (267)	400	Surface	
	T-10*	20.3 (199)	1 243	Root	
Small Test Piace	W-1	52.7 (516)	172	Root (blowhole)	0.8×1.0
	W-2	48.8(478)	2 126 →		
	W-3	50.7 (497)	898 →		
	W-4	51.7 (507)	1 616	Root	
	W-5	53.7 (526)	863	Root (blowhole)	0.3×0.3
	W-6	55.7 (546)	721	Root (blowhole)	0.1×0.4
	W-7	58.7 (575)	306	Root (blowhole)	0.2×0.5
	W-8	61.7 (605)	215	Root	
	W-9	63.7 (624)	139	Root (blowhole)	0.1×0.2
	W-17*	56.7 (556)	463	Root	
	W-18*	61.7 (605)	31	Root (blowhole)	0.6×0.8
	W-25*	53.7 (526)	773	Root	
	W-26*	56.7 (556)	523	Root (face)	
	W-27*	61.7 (605)	218	Root	
	W-30*	53.7 (526)	248	Root (blowhole)	0.4×0.6

* : beach mark test
→ : not failure

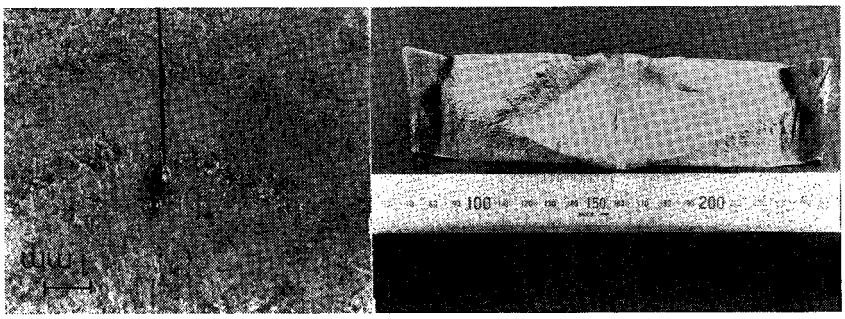

Photo 1 Fracture Surface of T-2 Large Specimen.

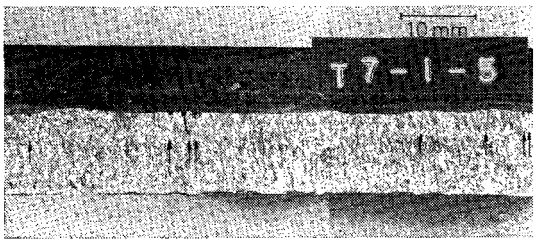

Photo 2 Configuration of Weld Metal at Root and Small Blowholes.

initiation of other large specimens were grinder scratch at surface [T-1], small pit at welding surface [T-4], and defect at part of repairs in base metal by welding [T-9, See 4, **Photo 5** and **Fig. 8**].

With all of the small test pieces, fatigue cracks were initiated from root portions of welds. There were small blowholes at the fracture surfaces of five test pieces. However, the sizes of blowholes were smaller than those in large specimens as was expected, because all of the small test pieces were made from one large specimen and the dimensions of the small test pieces were extremely small as compared with those of the large specimen. Consequently, the differences in fatigue strengths of large specimens and small test pieces in this study were caused by existence of welding residual stresses and sizes of blowholes.

Figs. 3, 4 shows the results of fatigue tests

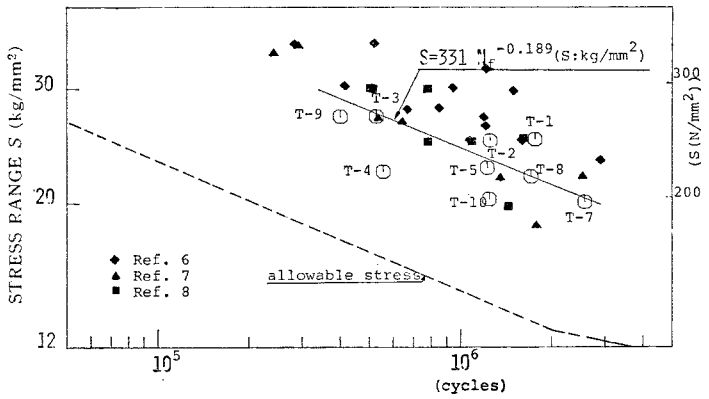

NUMBER OF CYCLES TO FAILURE N_f

Fig. 3 Fatigue Test Results of Large Specimens.

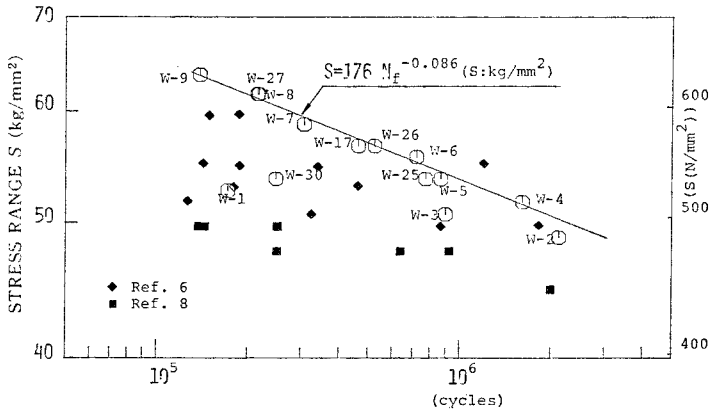

NUMBER OF CYCLES TO FAILURE N_f

Fig. 4 Fatigue Test Results of Small Test Pieces.

plotting stress range S on the ordinate and failure life N_f on the abscissa, both on logarithmic scales. The S-N_f curve calculated using a least squares fit for constant stress amplitude tests results is shown in **Figs. 3, 4**. In doing so, those in which fatigue cracks were not initiated from weld roots were omitted from the calculations. With specimens on which beach mark test were carried out, the testing stresses (the higher stress amplitude) and the number of cycles to failure (the number of cycles excluding the period of stress fluctuation reduced to one half) are plotted in **Figs. 3, 4**. There were large differences between the fatigue strengths of small test pieces and of large specimens, this trend being the same as stated in previous reports[6),8)].

The results on specimens in Refs. 6), 7) and 8) are also plotted in this figure. Welding of these specimens were done manually, the width and thickness of the parallel portions of the joint specimens were 70×14, 70×15 and 100×14 (mm), respectively, and the dimensions and the configurations of the small test pieces were the same as those in the study. The fatigue strengths of the large specimens were slightly lower than of those in the previous study. However, the fatigue strengths of the small test pieces in this study were higher than in the previous study.

The broken line in **Fig. 3** shows the current allowable stress for this type of joint under pulsating stresses for the Honshu-Shikoku bridges, and it may be seen that all of the test results satisfy the requirement of this criterion.

Fig. 5 shows the residual stress distributions in the direction of welding measured at the surfaces of unloaded large specimens. There are residual tensile stresses at weld metal portions and their vicinities. **Fig. 6** shows the residual stresses measured after fatigue tests. The residual tensile stresses were somewhat low compared with those in unloaded specimens.

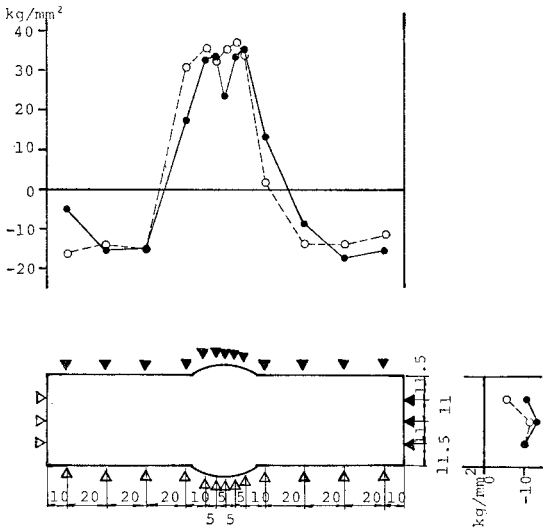

Fig. 5 Residual Stress Distribution in Unloaded Specimen.

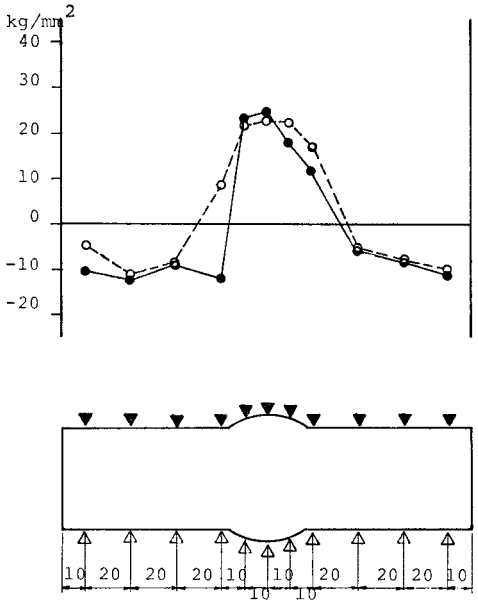

Fig. 6 Residual Stress Distribution in the Specimen after Fatigue Test.

4. INITIATION AND PROPAGATION OF FATIGUE CRACKS

A beach mark expresses the configuration of a fatigue crack at the time of variation in stress conditions. **Photo 3** shows a fracture surface with beach marks and **Fig. 7** shows the stress history and the results of observations of beach marks of the large specimen, T-8. A fatigue

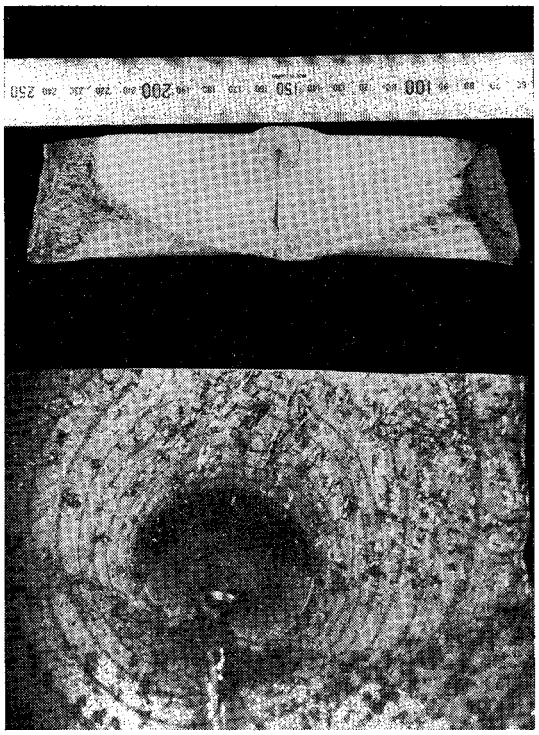

Photo 3 Fracture Surface with Beach Marks of T-8 Specimen.

crack had been initiated from the wall of a blowhole at the weld root. In this specimen, the number of times of reduction to one half of the stress range is 34, from which 30 beach marks were left on the fracture surface. Therefore, it is clear that the first beach mark had been formed by the fifth halving of the stress range and the fatigue crack had been initiated and started to propagate after the number of cycles of testing stress (nt) had reached 2×10^5 cycles and before it reached 2.5×10^5 cycles. Accordingly, if crack initiation life (N_c) is defined as the number of cycles of testing stress until formation of the first beach mark, N_c/N_f of this specimen is 0.12. However, because the spaces between the first and second beach marks and the third and fourth beach marks are wide compared with others, it is thought that distinct beach marks were not formed between them in spite of halving of the stress range. Consequently, it is surmised that the fatigue crack was initiated at the extremely early stage of repetitive stressing.

Photo 4 shows fractographs of Specimen T-8 obtained by scanning electron microscope. There is one micro crack at the corner of the blowhole. However, the fatigue crack was initiated from irregularities in the surface of the blowhole.

In **Fig. 3**, the results of Specimen T-8 are

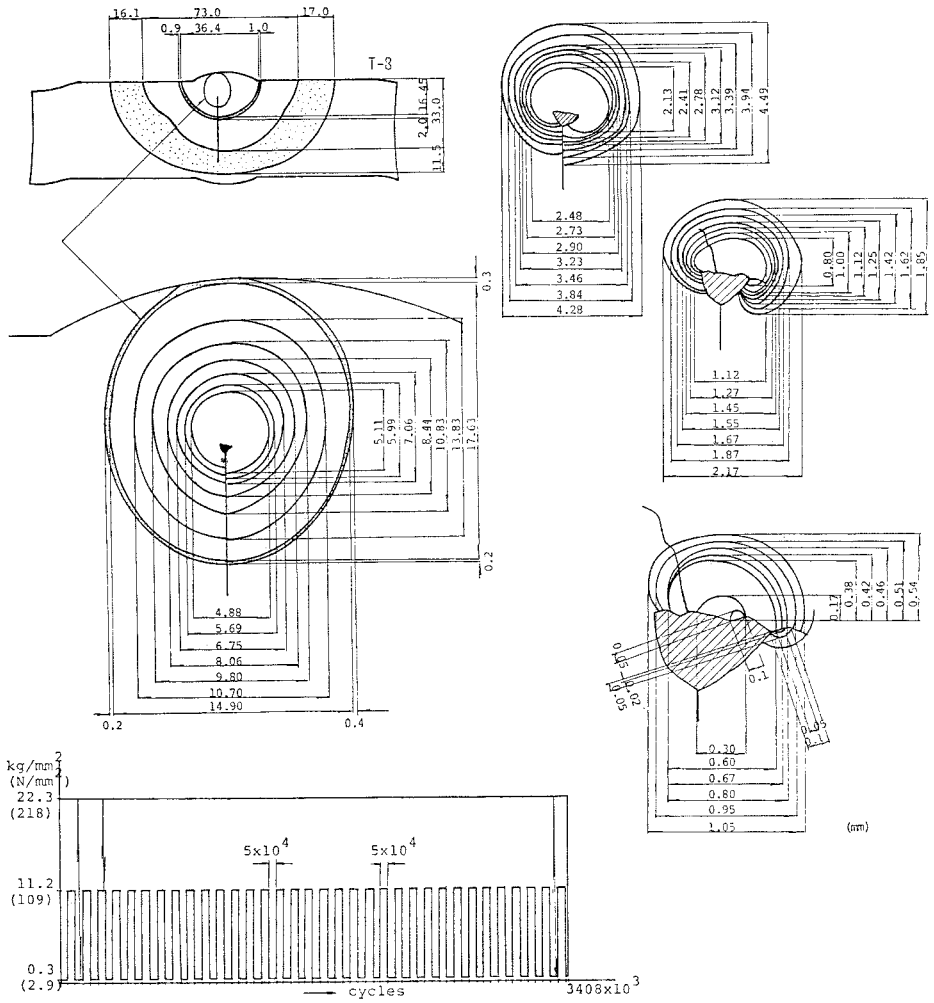

Fig. 7 Stress Histories and Observations of Beach Marks of T-8 Specimen.

nearly plotted on the S-N curve obtained from constant stress range tests. Therefore, with most of the large specimens on which constant stress range tests were performed, it is surmised that fatigue cracks were initiated and began to propagate at extremely early stages of stress repetitions similarly to Specimen T-8.

Photo 5 and **Fig. 8** shows the results of beach mark tests of the large specimen, T-9. With this specimen, one fatigue crack [Crack I] was initiated from a defect like a blowhole existing at a part of repair made on base metal by welding, which was propagated to result in failure. This repair is thought to have been made at the time of fabrication of the specimen. The dimensions of the repairing weld of 10 mm and depth of 3 mm. Consequently, it may be expected that there are considerably large welding residual stresses at these portions.

This specimen was failured during the eighth stress amplitude halving period, and there were 7 beach marks left on the fracture surface. Accordingly, it is considered that this fatigue crack was initiated before application of testing stresses reached 5×10^4 cycles.

There was another fatigue crack [Crack II] on this fracture surface which was initiated from pitting formed in welding. Six beach marks were observed in this fatigue crack plane. Accordingly, it is clear that this crack was also initiated at an early stage of life.

The results of beach mark tests of Specimen T-10 are shown in **Photo 6** and **Fig. 9**. The fatigue crack was initiated from the root of welding. However, because of stepping at the root which might have been caused by initiation of plural fatigue cracks, detailed observations of the portion of crack initiation were not possible.

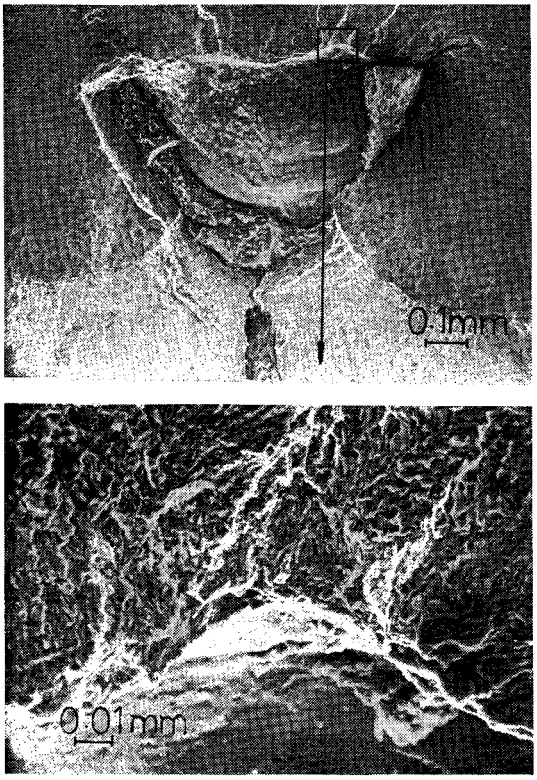

Photo 4 Fractographs of T-8 Specimen by SEM.

This specimen was subjected to a total of six stress range reductions to one half, from which six beach marks were left on the fracture surface. Therefore, the first beach mark was formed by the first halving of the stress range and it is clear that this fatigue crack was initiated before 2×10^5 cycles of testing stress. In **Fig. 3**, the results for Specimen T-10 are plotted considerably below the S-N curve.

The configurations of the fatigue cracks of Specimen T-8 were roughly semi-circular until crack lengths became equal to the width of the blowhole, following which, the fatigue cracks grew into a circle to surround the blowhole. Just before the fatigue crack appeared at the surface of the specimen, the cracks formed an ellipse. The dimensions of beach marks measured are indicated in **Fig. 10**. **Fig. 11** shows the dimensions of beach marks (a) of T-8 and T-10 large specimens at which they were plotted with the abscissa as "nt/N_f" (nt: the number of cycles of testing stress to form individual beach mark, N_f: the number of cycles of testing stress to failure) and ordinate as "a". The distance from the location of fatigue crack initiation to the surface of specimen is about 10 mm, therefore the fatigue crack appear at the surface of specimen at $a=10$ mm.

Photo 5 Fracture Surface with Beach Marks of T-9 Specimen.

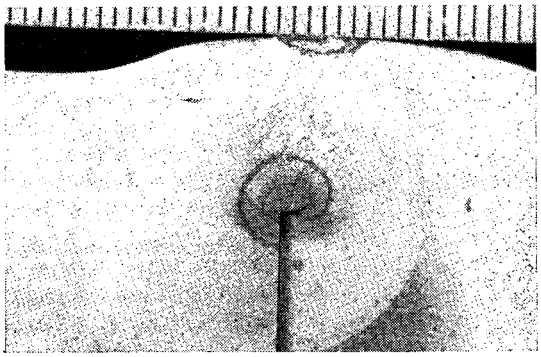

Photo 6 Fracture Surface with Beach Marks of T-10 Specimen.

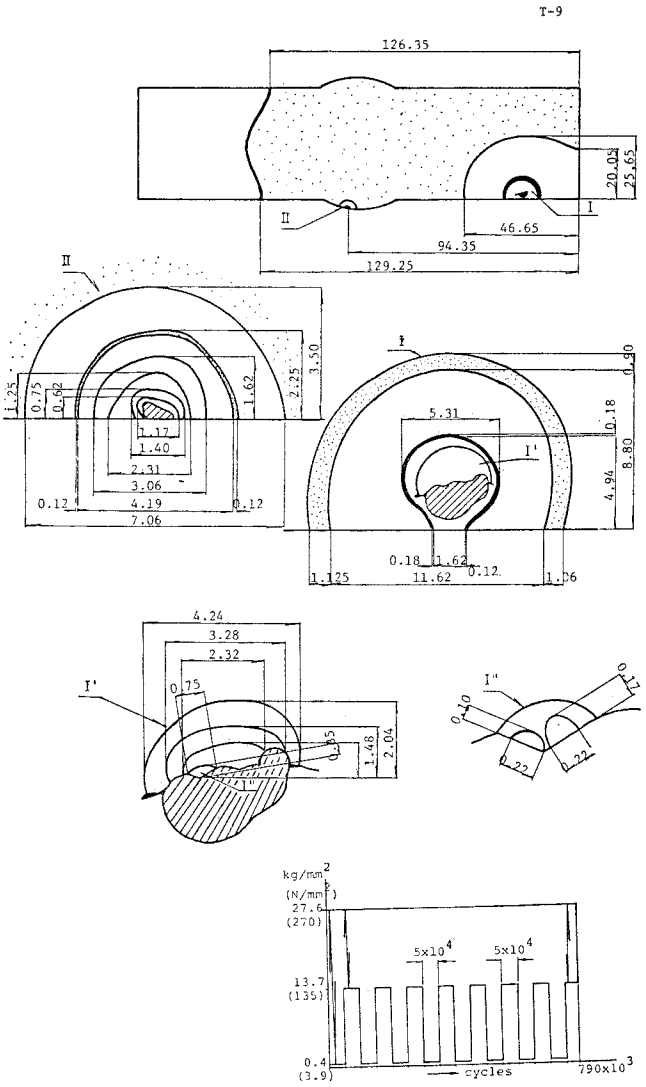

Fig. 8 Stress Histories and Observation of Beach Marks of T-9 Specimen.

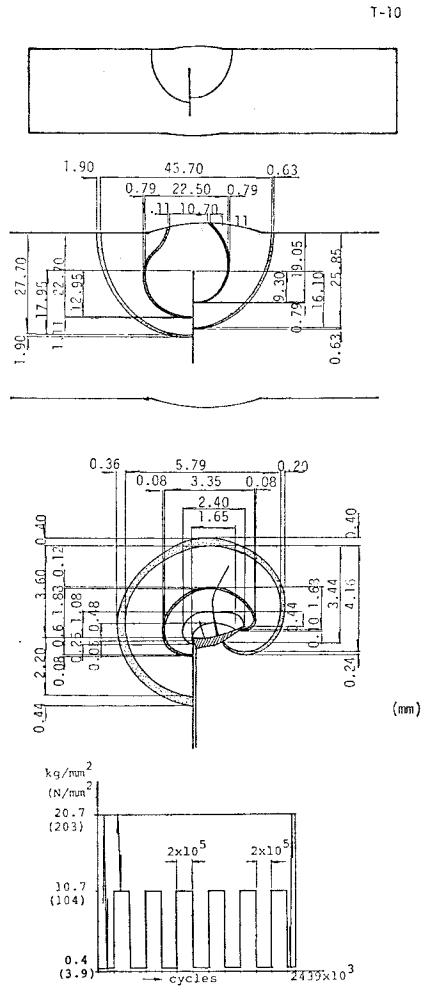

Fig. 9 Stress Histories and Observations of Beach Marks of T-10 Specimen.

From this figure, the times at which fatigue crack appear at the specimen surface is at 90% of the failure life of T-8, 85% of that of T-10, while approximately 50% of the failure life is spent for the fatigue crack to propagate to radius of about 1 mm of T-8, 2 mm of T-10 Specimen.

Figs. 12~15 gives the results of beach mark tests of small test pieces. With test piece W-18 and W-30, similarly to the cases of the T-8 large specimens a fatigue crack was initiated from a blowhole at the weld root, and there was coincidence between the number of times of stress range halving and the number of beach marks. Therefore, the fatigue cracks of these test pieces were initiated at an extremely early stage of repetitive stressing.

Fig. 10 Dimension of Beach Mark (a).

With test piece W-25 and W-27, a blowhole could not observe in the fracture surface. The fatigue cracks of both test pieces were initiated from small irregularities at the bottom surface

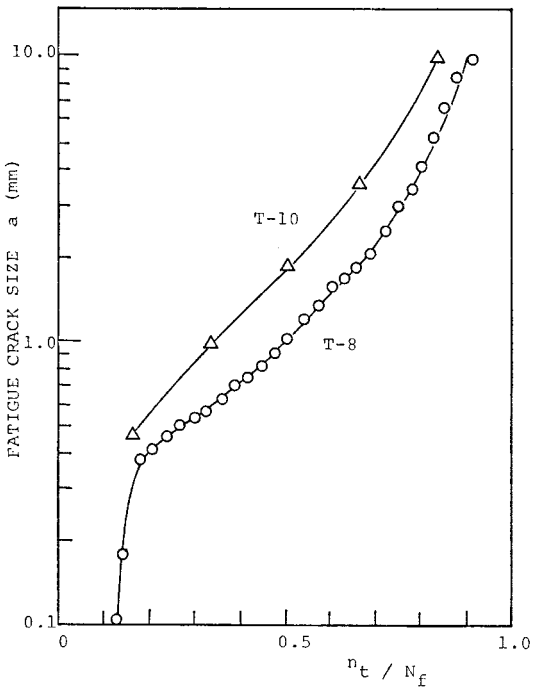

Fig. 11 Fatigue Crack Propagation from Weld Root to Surface.

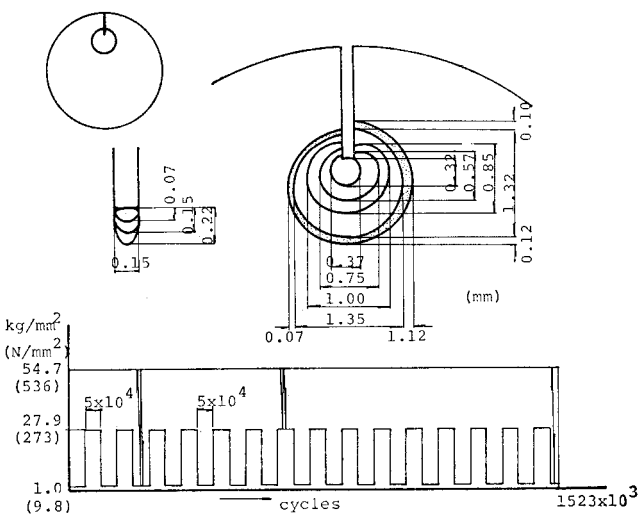

Fig. 13 Beach Mark Test Results of W-25 Test Piece.

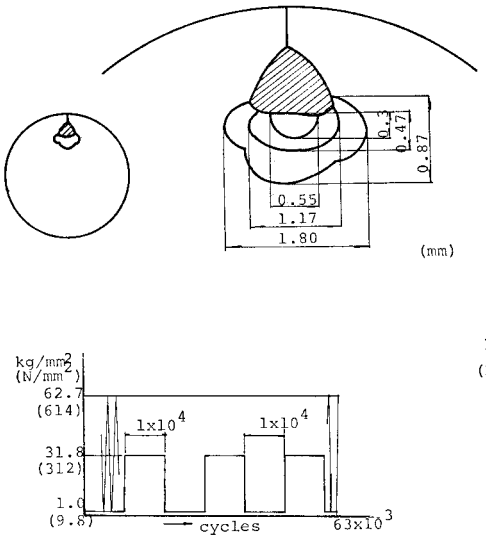

Fig. 12 Beach Mark Test Results of W-18 Test Piece.

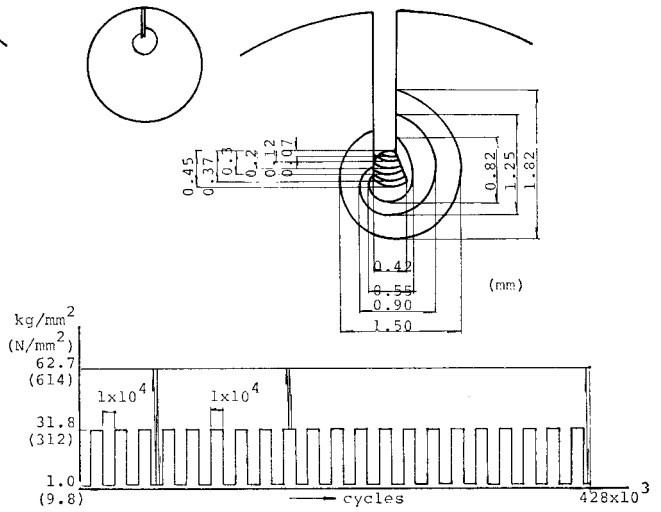

Fig. 14 Beach Mark Test Results of W-27 Test Piece.

of weld metal at the weld root. In these cases, a fairly large number of stress repetitions was required until fatigue cracks were initiated, and N_0/N_f was 0.35 and 0.57 respectively. From these test results, it may be predicted that fatigue life of this type of joint will be improved if welding is done without blowhole at the root.

5. ESTIMATION OF FATIGUE CRACK PROPAGATION LIFE

In view of the fact that the greater part of the fatigue life of this type of joint is spent in propagation of the penny-shaped fatigue crack, the

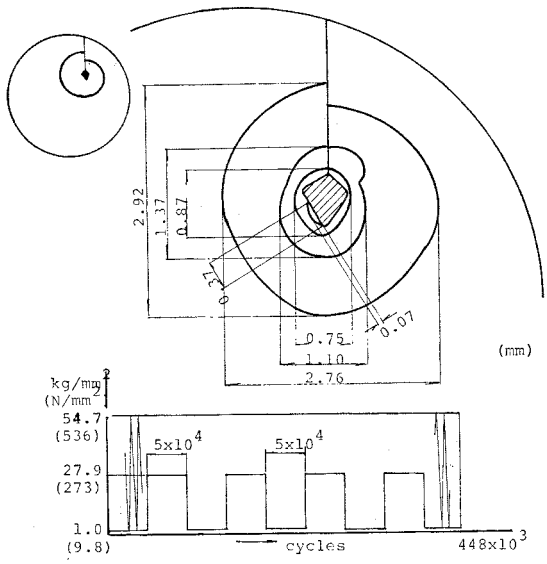

Fig. 15 Beach Mark Test Results of W-30 Test Piece.

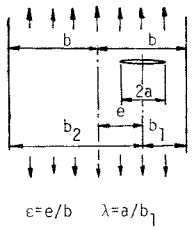

Fig. 16 Eccentric Crack.

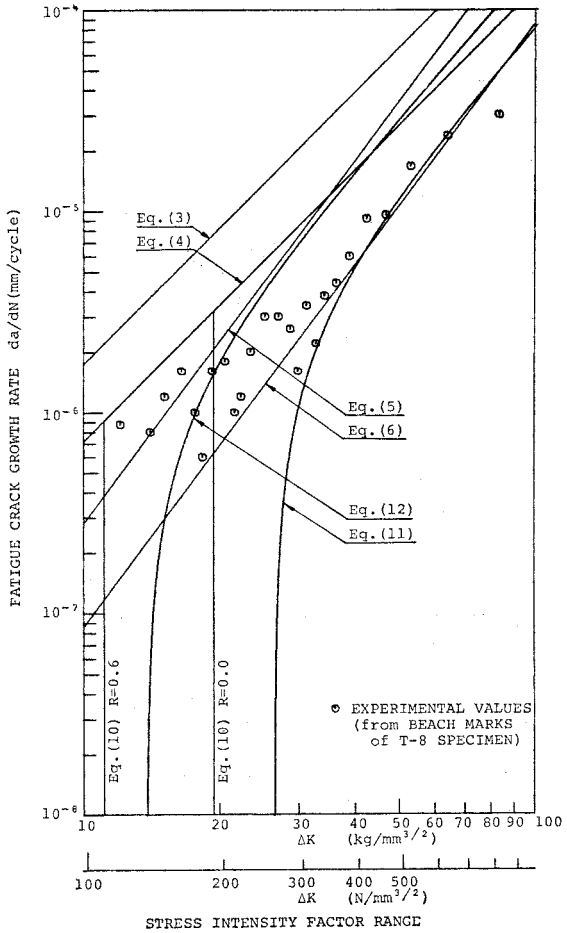

Fig. 17 Fatigue Crack Growth Rate Relationship of Eqs. (3)–(6), (11) (12) and Experimental Values from Beach Marks Spacing.

estimation of the fatigue crack propagation life of this was attempted employing fracture mechanics.

When the configuration of a fatigue crack initiated at the root is considered as a circle of radius a, the range of the stress intensity factor for this may be expressed by the equations below. $2/\pi$ of F is the correction factor for a penny-shaped crack and the rest of F are the correction factor for a eccentric crack in finite thickness plate[10] (**Fig. 16**).

(S: Stress range)

$$\left.\begin{aligned} \Delta K &= S\sqrt{\pi a}\cdot F \\ F &= \frac{2}{\pi}\sqrt{\sec\left(\frac{\pi\lambda}{2}\right)}\sqrt{\frac{\sin 2\lambda\varepsilon}{2\lambda\varepsilon}} \end{aligned}\right\} \cdots\cdots (1)$$

It is a well-known fact that Paris-law[11] of Eq. (2) is valid between fatigue crack growth rate (da/dN) and stress intensity factor range.

$$da/dN = C(\Delta K)^m \cdots\cdots (2)$$

Barsom[12] and others have arranged the results of fatigue crack propagation tests of various high tensile strength steels (yield stress σ_y not less than 56 kg/mm²) and obtained the following relationships:

Upper Limit of Crack growth rate.

$$da/dN = 9.7\times 10^{-9}(\Delta K)^{2.25} \cdots\cdots (3)$$

Lower Limit of Crack growth rate.

$$da/dN = 4.0\times 10^{-9}(\Delta K)^{2.25}, \quad \Delta K = \text{kg/mm}^{3/2} \cdots\cdots (4)$$

Maddox[13] sorted the results of fatigue crack Propagation experiments of base metal (σ_y= 38.8 kg/mm), weld metal (σ_y=39.4–64.9 kg/mm²) and heat affected zone and obtained the relationships below.

Upper Limit of Crack growth rate.

$$da/dN = 2.8\times 10^{-10}(\Delta K)^{3.0} \cdots\cdots (5)$$

Lower Limit of Crack growth rate.

$$da/dN=8.5\times10^{-11}(\Delta K)^{3.0},\quad \Delta K=\mathrm{kg/mm^{3/2}} \qquad \cdots\cdots(6)$$

Eqs. (3)~(6) are shown in **Fig. 17**. These equations were often used for the prediction of fatigue life of structures. As for the results of the beach mark tests on Specimen T-8, assuming that the crack configuration is a semi-circular or a circular, the relation of ΔK determined applying Eq. (1) and da/dN calculated from beach mark spacing was plotted in **Fig. 17**. The experimental values are distributed roughly between Eqs. (5) and (6).

Substituting into Eqs. (1) and (2), the following differential equation is obtained.

$$da/dN=C(S\sqrt{\pi a}\cdot F)^m \qquad \cdots\cdots(7)$$

The number of repetitions required for crack dimensions to develop from a_1 to a_2, namely, the fatigue crack propagation life (N_p) is obtained by Eq. (7) as shown below.

$$C(S)^m\cdot N_p=\int_{a_1}^{a_2}\frac{1}{\sqrt{\pi a}\cdot F}\cdot da \qquad \cdots\cdots(8)$$

If for a certain joint a_1 and a_2 are constant, and if F is constant, the right side of Eq. (8) will be constant, and the form of the so-called S-N line where the stress range and life become a straight line in the form of a logarithm as in Eq. (9) is obtained, and the gradient is $1/m$.

$$S=A\cdot N_p^{-(1/m)} \qquad \cdots\cdots(9)$$

where

A: constant

The results carrying out calculations by Eq. (8) under the conditions below are indicated in **Figs. 18** and **19**.

(i) Initial Crack Size a_1: 0.3 mm in large specimen and 0.2 mm in small test piece referring to blowhole dimensions at fracture surface. The initial crack size is very important for the fatigue life, but unfortunately it is very difficult to establish. These value of a_i are about the width of blowhole at the fracture furface (see **Table 3**) and larger than the radius of inscribed circle a little. Hirt and Fisher[15] have studied about some initial crack-models for weld defect and demonstrated that the shortest life estimates resulted from the circumscribed crack and longest from the inscribed crack.

(ii) Final Crack Size a_2: 8 mm in large specimen and 3 mm in small test piece. N_p is insensitive to a_2.

(iii) Stress intensity factor: According to Eq. (1). $2b=45$ mm, $e=12.5$ mm in large specimen and $2b=8$ mm, $e=0$ in small test piece.

(iv) $da/dN-\Delta K$: Eqs. (3)~(6) employed.

The test values obtained with large specimens are roughly scattered between the estimated life curves employing the propagation curves (Eqs. (5), (6)) according to Maddox. The estimated life lines employing the propagation curves by Barsom (Eqs. (3), (4)) are considerably shorter than indicated by test values. The test values

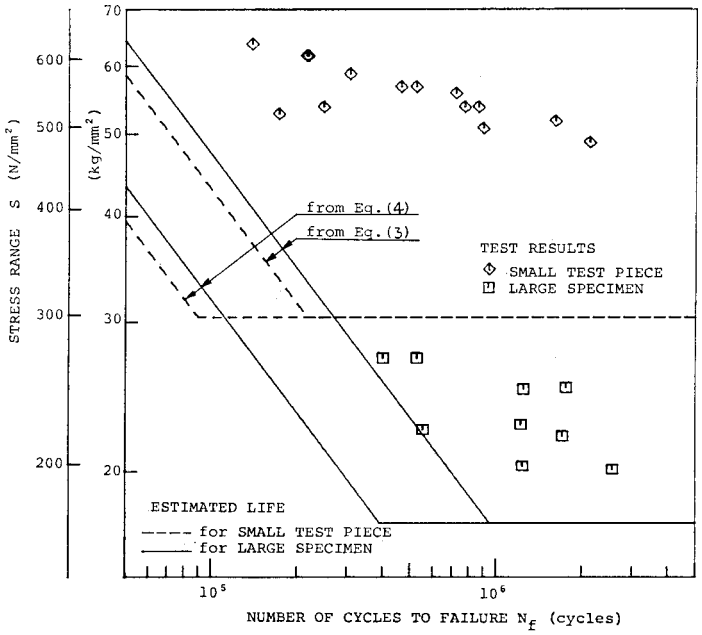

Fig. 18 Estimated Life from Eqs. (3), (4) and Fatigue Test Results.

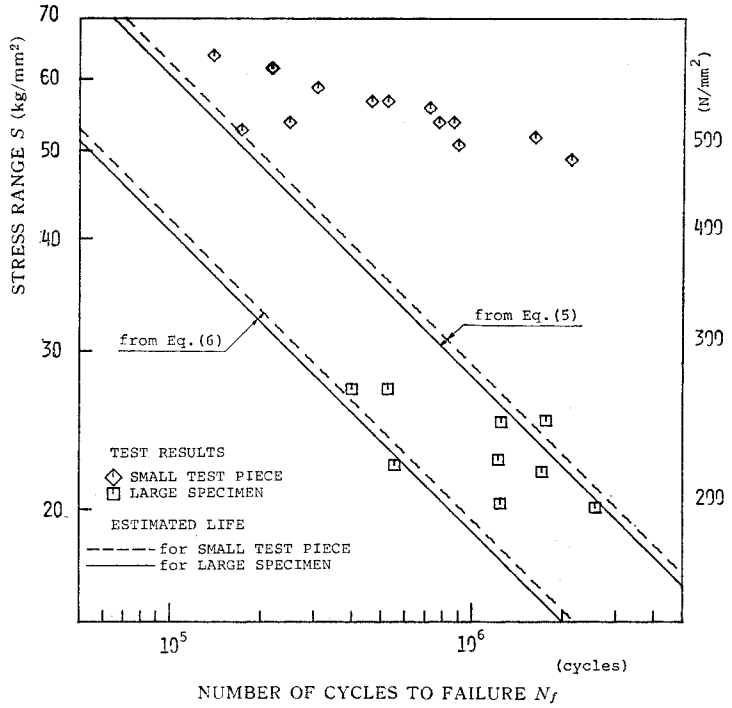

Fig. 19 Estimated Life from Eqs. (5), (6) and Fatigue Test Results.

obtained with small test pieces are considerably different from all estimated life curves.

On inversely calculating "m" from the gradient of the S–N straight line of the experimental values, the results are $1/0.153=6.53$ from the straight line for the large specimen, and $1/0.086=11.6$ for the small test piece. Both values are considerably different from the m-value ontained from fatigue crack propagation experiments.

The fatigue crack growth rate, when the stress intensity factor range falls below a certain value, turns away from the relationship of Eq. (2) to abruptly become small, and reaches the threshold stress intensity factor range (ΔK_{th}). The range in which Eq. (2) is valid and ΔK_{th} are both influenched by the stress ratio R. The lower limit value of stress (S_l) during fatigue tests of the welded portion of a large specimen is the sum of residual tensile stress (S_{rd}) and minimum stress (S_{min}) according to fatigue tests, and the upper limit value (S_u) is the sum of S_{rd} and the maximum stress (S_{max}) according to fatigue tests. From **Fig. 5, 6**, based on the fact that S_{rd} is from 25 to 35 kg/mm² and on taking $S_{rd}=30$ kg/mm² and $S_{min}=0.1$ kg/mm² and calculating local stress ratio R using S_u and S_l, the results will be $R=0.54$ in case of $S_{max}=25$ kg/mm² and $R=0.60$ in case of $S_{max}=20$ kg/mm².

Barsom[12] suggested a conservative estimate for the ΔK_{th} value for martensitic steels, ferrite-pearlite steels and anstentic steels to be

$$\Delta K_{th}=22.6(1-0.85R) \quad [\mathrm{kg/mm^{3/2}}] \quad \cdots\cdots(10)$$

Eq. (10) is valid for $\geqq 0.1$: for stress ratios <0.1 a ΔK_{th}-value of 19.04 kg/mm$^{3/2}$ was suggested. These provide a lower bound for ΔK_{th} in the region between $R=0.0$ and $R=1.0$ for structural steels[16),17)]. Threshold stress range calculated using Eq. (10) for both type of specimen are shown in **Fig. 18**. Ota et al.[14] have proposed a fatigue crack growth relationship which took Δk_{th} and R into account. Eqs. (11), (12) are the relationships as derived from the mean regression curves of fatigue crack growth test data at $R=0$ and $R=0.6$ for 80 kg/mm² class high tensile strength steel.

$R=0$

$$da/dN=6.91\times10^{-10}(\Delta K)^{2.54}-2.82\times10^{-6} \quad \cdots\cdots(11)$$

$R=0.6$

$$da/dN=1.42\times10^{-9}(\Delta K)^{2.54}-1.11\times10^{-6} \quad \cdots\cdots(12)$$

Eqs. (11) and (12) are indicated in **Fig. 17**. The relationship of ΔK and da/dN obtained from beach marks is close to Eq. (11) with ΔK higher than 40 kg/mm$^{2/3}$. However, although Ota et al. obtainded $\Delta K_{th}=26$ kg/mm² with $R=0$, the experimental values indicate that fatigue cracks

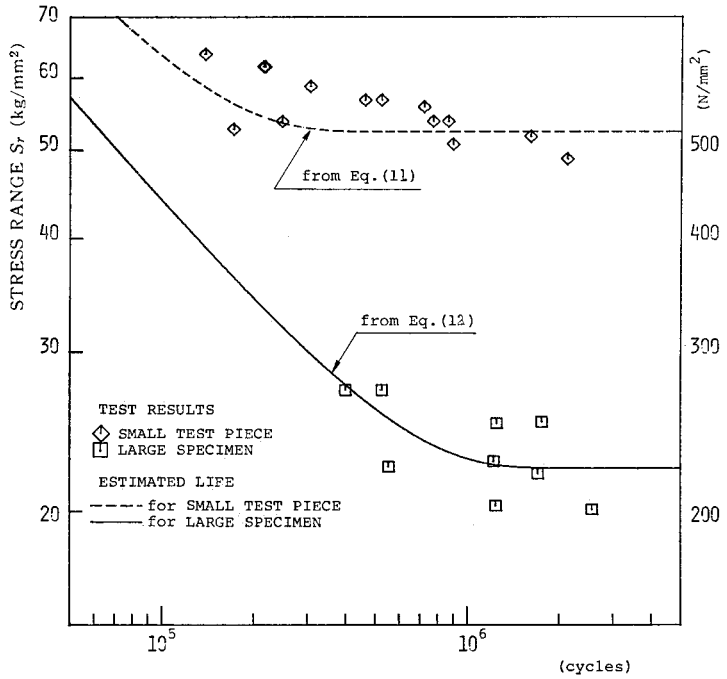

Fig. 20 Estimated Life from Eqs. (10), (11) and Fatigue Test Results.

progressed even at values of ΔK which were lower than ΔK_{th}, and on the whole, the experimental values are close to Eq. (12). It may be considered that the existence of residual welding stress has an effect similar to rise in the stress ratio for the fatigue crack growth rate.

The estimated life curves calculated using Eq. (12) for large specimens and Eq. (11) for small test pieces with regard to the relation between da/dN and ΔK and with other conditions the same as before are the curves in **Fig. 20**. The estimated curves using Eqs. (11) and (12) are very close to the experimental values for both large specimens and small test pieces.

Most of the life was exhausted while growth occured in a region of small ΔK. With T-8 specimen, about 75 parcent of the life was spent in region ΔK lower than 50 kg/mm$^{3/2}$ [500 N/mm$^{3/2}$], at growth rate was lower than 10^{-5} mm/cycle (See **Fig. 17**). Eqs. (3)~(6) were derived from the growth-rate data, the major part of that were higher than 10^{-5} mm/cycle. Careful evaluation of the crack grown relationships near the threshold stress intensity factor range is needed for the appropriate prediction of fatigue life.

6. CONCLUSIONS

The principal results obtained in the study are as follows.

(1) The fatigue strengths of the large specimens were slightly lower than those of common-size specimens in the previous study, but all of the test results satisfy the requirement of the current allowable stress for this joint for the Honshu-Shikoku Bridges. The fatigue strengths of the small test pieses were very high, and there were large differences between the fatigue strengths of small test pieces and of large specimens.

(2) The starting points of fatigue cracks in six out of the entire nine large specimens were blowholes existing at weld roots. The size of blowholes in the small test pieces were smaller than those in large specimens. Consequently, the differences in fatigue strengths of large specimens and small test pieces in this study were by existence of welding residual stresses and size of blowholes.

(3) With large specimens, fatigue crack were initiated and began to propagate at extremely early stage of stress repetitions. Fatigue cracks initiated at weld roots are propagated while becoming circular. Fatigue cracks appear at specimen surfaces on roughly 85%~95% of failure life, while approximately 50% of the failure life is spent for the fatigue crack to propagate to radius of 1~2 mm.

(4) The estimated life curves obtained based

on the following assumptions are very close to the experimental values.

(i) The initial defect is assumed to be a penny-shape crack which simply continues to develop in that form.

(ii) The influences of residual stress on the fatigue crack growth rate and threshold stress intensity factor range are equal to the influence of stress ratio.

7. ACKNOWLEDGEMENTS

The authors express their gratitude to Professor Dr. T. Nishimura of Gunma University for valuable suggestions.

The authors would like to thank Messrs. Y. Eguchi and H. Tanifuji (The Japan Construction Method and Machinery Research Institute), M. Tsurumaki (Tokyo Institute of Technology), for their assistance with the experimental work and preparation of the paper.

8. NOMENCLATURE

S: stress range.
N_f: failure life.
N_c: crack initiation life.
N_p: fatigue crack propagation life.
n_i: number of cycles of testing stress, excluding the period of stress range reduced in half.
a: crack size.
ΔK: stress intensity factor range.
da/dN: fatigue crack growth rate.
c, m: constants of Paris-law.
R: stress ratio, minimum stress/maximum stress in fatigue test.
ΔK_{th}: threshold stress intensity factor range.

REFERENCES

1) Japan Society of Civil Engineers: Fatigue Design for Honshu-Shikoku Bridges, 1974 (in Japanese).
2) Japan Society of Civil Engineers: The Specifications of Steel Railway Bridges, 1974 (in Japanese).
3) Tajima, J., A. Okukawa, M. Sugizaki and H. Takenouchi: Fatigue Tests of Panel Point Structures of Truss made of 80 kg/mm² High Tensile Strength Steel, IIW. Doc. No. XIII–831–77, July 1977.
4) Tajima, J., A. Okukawa and H. Takenouchi: Fatigue Tests of Panel Point Structures of Truss, Proceedings of 32nd Annual Meeting of JSCE, I–326, 1977 (in Japanese).
5) Honshu-Shikoku Bridge Authority, No. 272.–232–1 (4), June, 1980 (in Japanese).
6) Nishimura, T., J. Tajima, A. Okukawa and C. Miki: Fatigue Strength of Longitudinal Single-Bevel-Groove Welded Members, Proceedings of JSCE, No. 291, pp. 27～40, 1979-11 (in Japanese).
7) Nishimura, T. and C. Miki: Fatigue Strength of Longitudinal Welded Members of 80 kg/mm² Steel, Technical Report No. 22, Department of Civil Engineering, Tokyo Institute of Technology, pp. 1～27, Jan. 1978 (in Japanese).
8) Miki, C., F. Nishino, J. Tajima and Y. Kishimoto: Initiation and Propagation of Fatigue Cracks in Partially-Penetrated Longitudinal Welds, Proceedings of JSCE, No. 312, pp. 129～140, Aug. 1981.
9) Ito, F. and Y. Eguchi: Fatigue Tests of Large-size Longitudinal groove Welds of Quenched and Tempered 80 kg/mm² Steel, Hurried Report of the Railway Technical Research Institute, Japanese National Railways, 1967-4 (in Japanese).
10) Ishida, M.: Stress Intensity Factors for the Tension of an Eccentrically Cracked Strip. Journal of Applied Mechanics, Trans. ASME, pp. 674～675, Sept. 1966.
11) Paris, P.C. and F. Erdogan: A Critical Analysis of Crack Propagation Laws, Journal of Basic Engineering, Trans. ASME. 85, No. 3, 1163.
12) Rolfe, S. T. and J. M. Barsom: Fracture and Fatigue Control in Structures Prentice-Hall, Inc., pp. 236～239, 1977.
13) Maddox, S. J.: Assessing the Significance of Flaws in Welds Subject to Fatigue, Welding Journal, 53, No. 9, Sept. 1974.
14) Ota, A., E. Sasaki and M. Kosuga: Effect of Stress Ratios on the Fatigue Crack Propagation Rate, Transactions of the Japan Society of Mechanical Engineers, Vol. 43, No. 373, pp. 3173～3191, 1977 (in Japanese).
15) Hirt, M. A. and J. W. Fisher: Fatigue Crack Growth in Welded Beams, Engineering Fracture Mechanics, Vol. 5, pp. 415～429, 1973.
16) Hausamman, H.: Infulence of Fracture Toughness on Fatigue Life of Steel Bridges, Ph. D. Dissertation, Lehigh University, 1980.
17) Yamada, K., T. Makino, C. Baba and Y. Kikuchi: Proceedings of JSCE, No. 203, pp. 31～41, 1980-11 (in Japanese).

(Received January 20, 1981)